 doi:10.20944/preprints202207.0128.v1

Article

Effect of Co and Cr on the Stability of Strengthening Phases in Nickelbase Superalloys

Martin Bäker* and **Joachim Rösler**

Institute for Materials Science, Technische Universität Braunschweig, Langer Kamp 8, D-38106 Braunschweig 1; martin.baeker@tu-braunschweig.de; j.roesler@tu-braunschweig.de

* Correspondence: martin.baeker@tu-braunschweig.de; Tel.: +49-531-391-3065

Abstract: Nickel-base superalloys like VDM 780 may possess a high content of Cr and Co. This influences solution energies of phase-forming elements like Al and Ta (γ'-phase), Nb (γ''- and δ-phase), and Ti (η-phase). We perform density functional theory studies of a nickel matrix at 0 K with high concentrations of either Co and Cr and calculate the influence of these elements on solution energies. In the case of Co, the solution energy can be predicted well by the nearest-neighbor interaction in the Co-rich matrix. For Cr, the effect is more complicated because Cr has a larger ionic radius and changes the magnetic state of the material. The effect of a Cr-rich matrix on the energy of Co is dominated by magnetic effects, interactions with the other elements by elastic deformation of the lattice.

Keywords: nickelbase alloys; phase stability; density functional theory

1. Introduction

Nickel-based superalloys possess an outstanding mechanical strength even at high temperatures due to the formation of the strengthening γ'- (Ni_3Al) and γ''-phase (Ni_3Nb). In wrought alloys, the δ- (Ni_3Nb) and η-phase (Ni_3Ti) are also important because they can be utilized to ensure a fine-grained structure, but also may form precipitations that embrittle the alloy during service [1].

To predict the behavior of these alloys, density functional theory calculations can be employed [2–7]. Usually, formation energies of the precipitation phases are calculated with respect to the energy of either the pure materials (e. g. Al in the case of γ') or with respect to the solution energy of the element under consideration in a nickel matrix. However, wrought alloys like VDM Alloy 780 [8] may contain a high amount of Co and Cr. The reference energy for the formation of one of the precipitate phases should thus be the energy of the element under consideration in a matrix that is rich in Co and Cr.

Here we perform density functional theory studies of the energy of the elements Al, Ti, Nb, and Ta in a nickel matrix with realistic concentrations of Co or Cr. In addition, we also study the case of Co in a Cr-rich matrix. We show that the solution energy can be understood simply by considering nearest-neighbor effects in a Co-rich matrix, whereas additional effects occur in a Cr-rich matrix. We also study the physical reason for the calculated energy changes.

2. Materials and Methods

All density functional theory calculations were performed using VASP with the PAW-PBE potentials [9–13]. For each element, the pseudopotential with maximum number of electrons was chosen. An energy cutoff of 520 eV and a first-order Methfessel-Paxton scheme with a smearing parameter of 0.07 eV were used. To ensure high precision, the precision parameter was set to "accurate", and real space projection operators were calculated to a precision of 10^{-4}. The convergence criterion for the electronic loop was set to 10^{-4} meV, the ionic loop during relaxation was stopped when the energy change was below 10^{-2} meV.

To calculate the correct volume of each supercell, the following procedure was used: In the first step, calculations with relaxation of the ionic positions and the cell shape were

Preprints (www.preprints.org) | NOT PEER-REVIEWED | Posted: 8 July 2022 doi:10.20944/preprints202207.0128.v1

done at fixed lattice volume for five different volumes. A Birch-Murnaghan state equation [14] was used to fit the energies and determine the optimum scale factor. For this scale factor, a final calculation was then performed with a k-point spacing of 0.1 $Å^{-1}$. Some intermediate calculations were performed using the simpler method of directly relaxing the cell shape, cell size and the ions.

Except for some auxilliary calculations described below, all calculations were spin-polarized. Ni atoms were usually initialized with a moment of $1\mu_B$, Co atom with a larger value. For cells containing Cr, different initializations of the magnetic moment of the Cr atom were tried because Cr can be antiferromagnetic in a nickel matrix. Details are described in the results section.

Calculations of the solution and nearest-neighbor interactions were performed using supercells with 108 atoms. For calculations with a high Co content, 64-atom special quasirandom structure (SQS) cells were created using the software ATAT [15]. For the Cr-rich matrix, calculations with 32-atom SQS cells were performed (the smaller size was chosen because converging to the correct magnetic state requires a large number of trial runs). In addition, cells with composition $Ni_{26}Cr_6$ and $Ni_{25}Cr_6X$ that contained no nearest-neighbor bonds between Cr atoms were created using the software tool SOD (Site-Occupation Disorder) [16].

3. Results

3.1. Influence of Co

3.1.1. Interaction effects at low concentrations

The first step in creating supercells with a high content of an alloying element like Co is to calculate the interaction energy of the element with itself when situated close in the lattice. If the energy of two alloying atoms increases strongly in a nearest-neighbor position, such configurations will not occur. On the other hand, attractive forces, for example on next-nearest neighbor positions, might lead to local ordering of the atoms.

The interaction energy $E_{\text{int, XY}}$ between two atoms X and Y in a certain configuration (nearest neighbor, next nearest neighbor etc.) is calculated by comparing supercells containing the atoms in this configuration with two supercells with isolated atoms. Using 108 atoms in the supercell, the interaction energy is

$$E_{\text{int, XY}} = E(\text{Ni}_{106}\text{XY}) + E(\text{Ni}_{108}) - (E(\text{Ni}_{107}\text{X} + E(\text{Ni}_{107}\text{Y}))\,. \tag{1}$$

Here, $E(\cdot)$ denotes the energy of the supercell. A negative interaction energy means that the configuration is energetically favorable, a positive energy means that separating the atoms is more favorable.

Using eq. (1), the interaction energy between Co and Co and between Co and the phase-forming elements (Al, Ti, Nb, Ta) can be calculated. Results are shown in table 1. The self-interaction of Co with itself is rather small, showing that Ni-Co bonds and Ni-Ni bonds have practically the same energy. Since the ionic radius of Co is almost identical to that of Ni, elastic interactions are negligible.

Placing one of the phase-forming elements next to Co has an energy cost of roughly 100 meV. There is no clear effect of the ionic radius of the elements because the lattice distortion is unchanged when one Ni neighbor is replaced by Co. Next nearest neighbor energies are generally negligible.

3.1.2. Interaction in Co-rich cells

Since there is no strong self-interaction of Co, a Co-rich nickel matrix will be disordered so that arbitrary configurations can be considered.

We created 3 special quasirandom structures, shown in Figure 1, using the program suite ATAT [15], with a composition of $Ni_{47}Co_{16}X$. To study the influence of high Co concentrations on the solution energy of an alloying element, we compare the energy of this cell with that of a cell where X is replaced with Ni. From this, the energy to transfer an

Preprints (www.preprints.org) | NOT PEER-REVIEWED | Posted: 8 July 2022 doi:10.20944/preprints202207.0128.v1

Table 1. Interaction energy between Co and other alloying atoms calculated in a matrix with 108 atoms. Energies shown are for nearest neighbor end next-nearest neighbor positions

Element	nearest neighbor	next nearest neighbor
Al	92.2 meV	0.0 meV
Ti	103.0 meV	2.7 meV
Co	1.3 meV	−3.5 meV
Nb	113.9 meV	3.7 meV
Ta	117.1 meV	1.5 meV

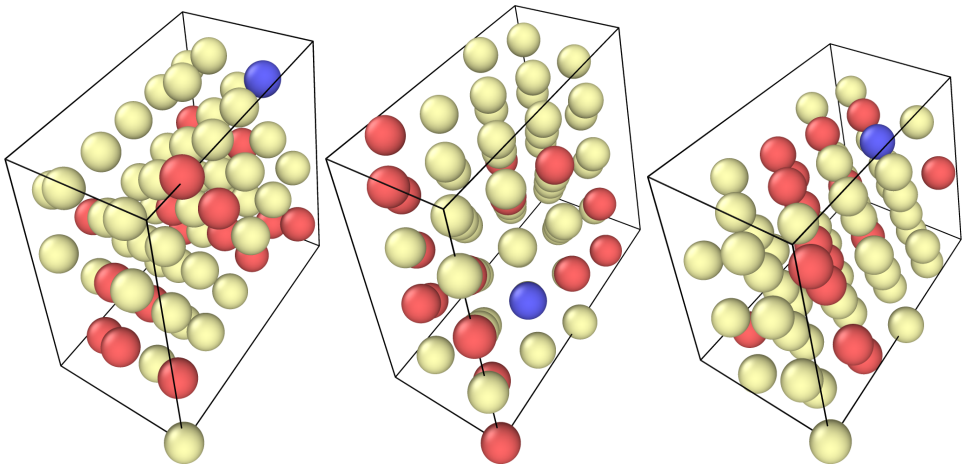

Figure 1. The 3 special quasirandom structures with composition $Ni_{47}Co_{16}X$; Ni atoms in yellow, Co atoms in red, alloying element in blue.

element from a pure nickel matrix to a matrix containing 25 at-% Co can be calculated as follows:

$$E_{\text{Co-rich,X}} = E(\text{Ni}_{108}) + E(\text{Ni}_{47}\text{Co}_{16}\text{X}) - (E(\text{Ni}_{107}\text{X}) + E(\text{Ni}_{48}\text{Co}_{16}))\,. \tag{2}$$

If this number is positive, placing the atom in a Co-rich matrix is less favorable than in a pure Ni matrix, so Co will tend to displace the element to other phases.

The results in table 2 show that the energy is positive in all cases; thus placing an alloying element in a Co-rich matrix is unfavorable compared to a pure Ni matrix. The alloying atom has three Co-neighbors in the special quasirandom cell. We can account for this by adding 3 times the nearest-neighbor interaction energy to the second term

$$\begin{aligned} E_{\text{Co-rich, X, nn}} &= E(\text{Ni}_{108}) + E(\text{Ni}_{47}\text{Co}_{16}\text{X}) - (E(\text{Ni}_{107}\text{X}) + E(\text{Ni}_{48}\text{Co}_{16}) + 3E_{\text{nn}}) \\ &= E_{\text{Co-rich,X}} - 3E_{\text{nn}}\,. \end{aligned} \tag{3}$$

Table 2. Energy $E_{\text{Co-rich}}$ to transfer an element from a pure nickel matrix to a matrix containing 25 at-% Co. Also shown is the energy $E_{\text{Co-rich, nn}}$ that accounts for nearest neighbor effects. If this number is small, the effect of a Co-rich matrix is mainly governed by nearest-neighbor effects. All energies are given in meV.

Element	SQS 1		SQS 2		SQS 3	
	$E_{\text{Co-rich,X}}$	$E_{\text{Co-rich,X, nn}}$	$E_{\text{Co-rich,X}}$	$E_{\text{Co-rich,X, nn}}$	$E_{\text{Co-rich,X}}$	$E_{\text{Co-rich,X, nn}}$
Al	250.8	−25.8	305.7	29.1	293.5	16.9
Ti	272.8	−36.3	338.8	29.7	352.2	43.2
Nb	284.9	−56.9	325.2	−16.6	372.8	30.9
Ta	299.8	−51.6	344.9	−6.5	390.5	39.1

Preprints (www.preprints.org) | NOT PEER-REVIEWED | Posted: 8 July 2022 doi:10.20944/preprints202207.0128.v1

$E_{\text{Co-rich, X, nn}}$ thus quantifies the part of the transfer energy that is not explained by the nearest-neighbor interaction. As can be seen from table 2, this energy is small in most cases, the largest deviation being −56.9 meV. This shows that the energies in the Co-rich matrix can be predicted quite well by the nearest-neighbor interaction.

In summary, the effect of a Co-rich matrix is explained mainly by the nearest neighbor interaction. An increase in the Co concentration can therefore be expected to increase the energy of the alloying element in the nickel matrix so that the respective phase is stabilized and its solvus temperature increased.

3.2. Influence of Cr

3.2.1. Cr-Cr interaction at low concentrations

Experimentally, it is known that Cr preferably bonds to unlike atoms [17]. However, a calculation of the Cr-Cr nearest neighbor interaction energy in a Nickel matrix, performed identically to that in section 3.1.1, yields an interaction energy of −101 meV when the Cr atoms are initialized with opposite magnetic moments to each other, rendering this configuration favorable. (If the Cr atoms are initialized with magnetic moments parallel to each other and to that of the Ni atoms, the final state has identical moments on both atoms and an interaction energy of −19 meV.)

There are several possible explanations for Cr atoms not favoring nearest neighbor positions: In alloys with high Cr-content, the material is not ferromagnetic, so magnetic effects may change the nearest-neighbor interactions. Other configurations, for example next-nearest neighbor positions, may be more favorable as suggested by the existence of a Ni_3Cr DO_{22} phase [18]. Furthermore, at higher concentrations of Cr, more complicated interactions between the Cr atoms may make nearest neighbor positions unfavorable.

The next-nearest neighbor position is indeed even more favorable in a Ni matrix with an interaction energy of −173 meV when the Cr atoms have opposite magnetic moments to each other (the resulting state has moments of $\pm 1.59\mu_B$). A ferromagnetic final state (with magnetic moments of $+1.18\mu_B$) leads to an interaction energy of −104 meV; a state where both Cr have the same magnetic moment, but opposite to the Ni matrix (with magnetic moments of $-1.66\mu_B$) has an interaction energy of −119 meV. The differences between these three magnetic states also suggests that magnetic interactions play an important role.

To further study the magnetic effects, non-spin polarized calculations were performed for the supercells Ni_{108}, $Ni_{107}Cr$, and $Ni_{106}Cr_2$. If the nearest-neighbor interaction is calculated in this state, the value changes drastically to 260 meV, making a nearest-neighbor position highly unfavorable.

In conclusion, the Cr-Cr interaction has been shown to be complex: In a ferromagnetic Ni matrix, the nearest-neighbor position is energetically favorable, but a next-nearest neighbor position has an even lower energy and will thus be preferred. Furthermore, the interaction energy depends on the magnetic state of the Cr atoms. In an unmagnetic Ni matrix, Cr-Cr nearest neighbor interactions are unfavorable.

3.2.2. Interaction between Cr and other alloying elements at low concentration

The interaction energy between Cr and the other alloying elements was calculated in the same way as in section 3.1.1 and 3.2.1. In addition, non-spin polarized calculations were also performed to see the effect of magnetic interactions. Results are shown in table 3.

In both cases, the interaction between Cr and Co is small. For the other elements, the energies in the spin-polarized calculation are close to each other. However, the magnetic state is not the same in all cases: For Al and Ti, an antiferromagnetic moment of Cr is more favorable, whereas the energetically lowest state for Cr-Nb and Cr-Ta is ferromagnetic with the anti-ferromagnetic polarization of Cr having an interaction energy that is larger by about 80 meV in both cases. It should be noted that converging to the correct magnetic state is difficult in these cases and requires a correct initialization of the magnetic moments and the correct choice of the minimization algorithm. The calculation may converge to a

Preprints (www.preprints.org) | NOT PEER-REVIEWED | Posted: 8 July 2022 doi:10.20944/preprints202207.0128.v1

Table 3. Nearest-neighbor interaction energy between Cr and other alloying atoms calculated in a matrix with 108 atoms. Results for both spin-polarized and non-polarized calculations are shown. Also shown are the atomic volumes (in units $Å^3$) of the elements in a (spin-polarized) $Ni_{107}X$ cell, calculated by a Voronoi construction.

Element	magnetic	nonmagnetic	Volume
Al	140	270	11.109
Ti	155	371	11.264
Co	5.9	-35	10.795
Nb	146	435	11.541
Ta	160	446	11.557

state with a large ferromagnetic, large antiferromagnetic, or a very small moment on the Cr atom, so it seems that there are actually three local minima for the electronic state.

In the non-spin-polarized case, the interaction energy is generally higher. In this case, there is a good correlation between the interaction energy and the atomic volume of the alloying elements (calculated using a Voronoi construction), showing that the interaction energy is dominated by the elastic repulsion between large ions. In the magnetic case, the increased elastic energy is countered by lowering the energy due to the ferromagnetic Cr orientation when placed next to Nb and Ta.

3.2.3. Construction of $Ni_{26}Cr_6$ cells

To check the effect of large Cr concentrations, cells with composition $Ni_{26}Cr_6$, corresponding to a concentration of 18.75 at.-%, were created in two different ways.

Theresults from section 3.2.1 suggest that Cr-Cr nearest neighbor positions are less favourable than next-nearest neighbor positions and there is also experimental evidence that Cr atoms avoid these positions. (This is also corroborated by the fact that the energies of the SQS cells with Cr-Cr nearest-neighbor bonds that are discussed below are considerably larger.) Therefore, $Ni_{26}Cr_6$ cells with no Cr atoms in nearest neighbor positions were created using the software SOD [16]. The seven possible configurations are shown in Fig. 2. To ascertain the most favorable magnetic state of the cells, initial static calculations for each of the cells were performed where the magnetic moments of the Cr atoms were varied systematically. Afterwards, the most favorable magnetic state was used to initialize a calculation with relaxation of ions and cell size.

The most favorable configuration was configuration 7 where the Cr atoms form three independent chains when periodic boundary conditions are taken into account. Energies of the other structures were larger by energies of up to 649 meV.

In the most favorable structure, the Cr atoms in each chain have opposing magnetic moments, whereas the moments in the Ni matrix are small. To check whether this structure is most favorable due to this magnetic interaction, we performed another calculation with no spin polarization. The energy of this was larger by only 84 meV, considerably less than the energy difference to most of the other structures.

It is therefore most plausible that the energy of the $Ni_{26}Cr_6$ cell is mainly determined by elastic interactions between the Cr atoms. This is corroborated further by the fact that structures 1, 2 and 5, which have an $L1_2$-like structure with two Cr atoms replaced by Ni, have the highest energies. Since the ionic radius of Cr is larger than that of Ni, the Ni-Ni-bonds in positions where a Cr atom is "missing" are probably highly strained and thus increase the energy of the structure. The only exception to this is configuration 4 which is similar to configuration 3, but has a considerably higher energy.

We can also use these structures to further assert that Cr-Cr nearest neighbor bonds are unfavorable. To do so, one Cr atom in configuration 7 was shifted into a nearest neighbor position to the other atom on its chain while leaving the number of Cr-Cr atoms on next-nearest neighbor positions unchanged. The energy difference between these two configurations is 328 meV. This number is of the same order of magnitude as the

Preprints (www.preprints.org) | NOT PEER-REVIEWED | Posted: 8 July 2022 doi:10.20944/preprints202207.0128.v1

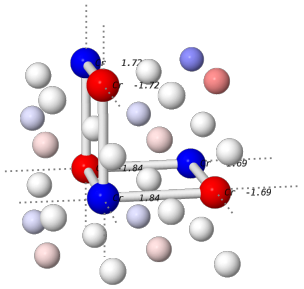

Configuration 1,
$\Delta E = 534\,\text{meV}$

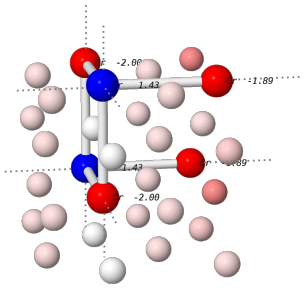

Configuration 2,
$\Delta E = 649\,\text{meV}$

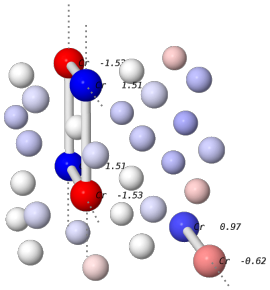

Configuration 3,
$\Delta E = 199\,\text{meV}$

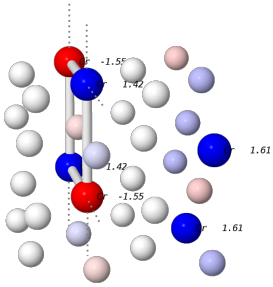

Configuration 4,
$\Delta E = 495\,\text{meV}$

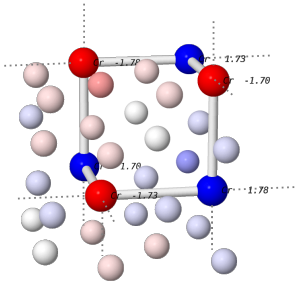

Configuration 5,
$\Delta E = 488\,\text{meV}$

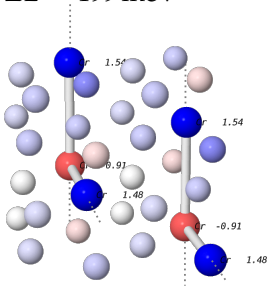

Configuration 6,
$\Delta E = 256\,\text{meV}$

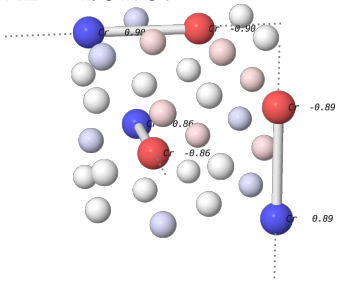

Configuration 7,
$\Delta E = 0\,\text{meV}$

Figure 2. The seven possible $Ni_{26}Cr_6$ supercells with no nearest-neighbor bonds between Cr atoms. Cr atoms are plotted with a larger radius. Next-nearest neighbor bonds inside the cell are shown, periodic nearest-neighbor bonds are depicted as dashed lines. The color of the atoms encodes the magnetic moments in the final state. Magnetic moments for the Cr atoms are listed in the plots. For all configurations, energy differences relative to the lowest-energy configuration 7 are stated.

Preprints (www.preprints.org) | NOT PEER-REVIEWED | Posted: 8 July 2022 doi:10.20944/preprints202207.0128.v1

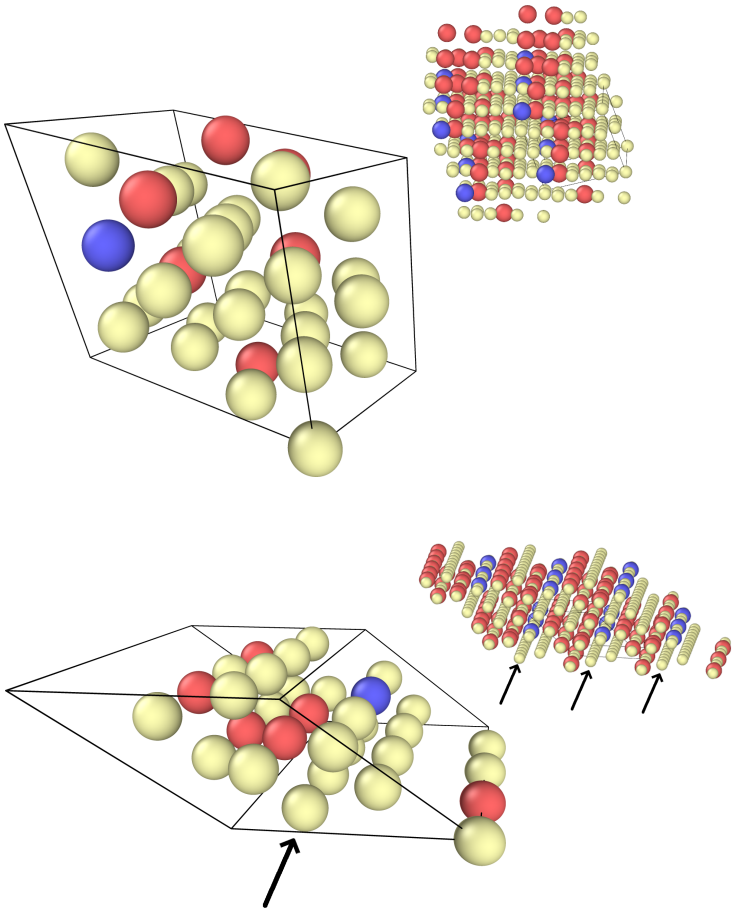

Figure 3. The two special quasirandom structures with composition $Ni_{25}Cr_6X$; Ni atoms in yellow, Cr atoms in red, alloying element in blue. The smaller pictures show a periodically repeated pattern, arrows in the second picture mark close-packed planes that do not contain Cr atoms.

nonmagnetic nearest-neighbor interaction energy calculated in section 3.2.1, showing that nearest-neighbor bonds between Cr atoms are indeed unfavorable.

In addition, we created two cells with a special quasirandom structure (SQS) for a composition of $Ni_{25}Cr_6X$ to be used in the calculations of the alloying element interactions [15]. Replacing the X atom with Ni leads to a $Ni_{26}Cr_6$ cell that serves as reference state for the alloying calculations. Using this procedure has the advantage that in calculating the alloying effects, two cells are compared that only differ by the replacement of a single Ni atom with an alloying atom, so that interactions between the Cr atoms remain the same. Fig 3 shows the SQS cells.

The energies of the two $Ni_{26}Cr_6$ SQS cells (with a Ni atom in place of the alloying atom) are considerably larger than that of the most favorable state from Figure 2 by 1 378 meV and 1 391 meV. In both cells, 64 initializations of the magnetic moments of the Cr atoms were tried to find the best magnetic state. In the first cell, three Cr atoms have positive magnetic moments, the other three have negative moments, and the magnetic moments on the nickel atoms are low overall, so that the net magnetic moment of the cell is small. In the second configuration, there are four Cr atoms with positive moments, leading to larger moments on the Ni atoms and a larger overall magnetic moment. It may seem surprising that the energies of both cells are very close despite magnetic interactions being larger in SQS 2. This is probably due to a cancellation of elastic and magnetic energies as will be discussed in the next section.

Preprints (www.preprints.org) | NOT PEER-REVIEWED | Posted: 8 July 2022 doi:10.20944/preprints202207.0128.v1

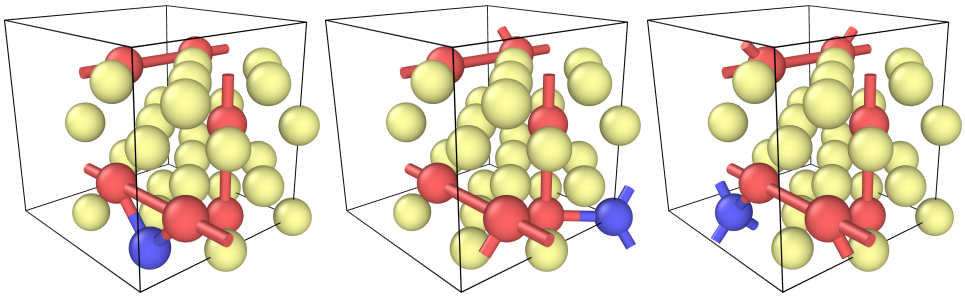

Figure 4. The three geometrically distinct positions of an alloying atom in the energetically best cell $Ni_{25}Cr_6X$ from figure 2. Nearest-neighbor bonds between the alloying atom and Cr and next-nearest-neighbor bonds between Cr atoms are shown. Ni atoms in yellow, Cr atoms in red, alloying element in blue.

3.2.4. Interaction in cells with high Cr content

Interaction effects were calculated for $Ni_{25}Cr_6X$ in the two SQS cells from Figure 3 and in the lowest energy cell without nearest neighbors, configuration 7 from Figure 2. There are three geometrically different positions in this cell as calculated using SOD [16], with 2, 3, and 4 nearest Cr neighbors of the alloying element. These cells are denoted as "non-nn-cells" in the following. In all cases, different initial magnetizations for the alloying element and the Cr atoms were used to find the best final state.

The energy to transfer an alloying element from a pure Ni-matrix to a Cr-rich matrix is calculated in the same way as in eq. (2):

$$E_{\text{Cr-rich,X}} = E(\text{Ni}_{108}) + E(\text{Ni}_{25}\text{Cr}_6\text{X}) - (E(\text{Ni}_{107}\text{X}) + E(\text{Ni}_{26}\text{Cr}_6)) \,. \tag{4}$$

A negative number means that placement in the Cr-rich matrix is more favorable, a positive number means that it is less favorable.

Table 4 shows the calculated transfer energy which is positive for all elements. This shows that a Cr-rich matrix will tend to displace the studied elements to other phases compared to a Cr-free Ni matrix. The absolute values vary strongly, but it should be noted that the energy of SQS 1 and non-nn-cell 1 are always rather close. Both these cells have two Cr-neighbors on the alloying atom. The transfer energy of SQS 2—which also has two nearest Cr neighbors—is consistently lower than that of SQS 1 by 120 meV–160 meV; reasons for this will be discussed below.

Apart from Co, which will be discussed separately, it is apparent that the transfer energy increases significantly with the number of nearest Cr-neighbors of the alloying atom. This suggests that nearest-neighbor effects play some role in determining the energy of the alloying atom. To account for this, we can subtract the nearest-neighbor interaction energy as in eq. (3) and calculate

$$E_{\text{Cr-rich,X, nn}} = E_{\text{Cr-rich,X}} - N_{\text{nn}} E_{\text{nn}} \,, \tag{5}$$

where N_{nn} is the number of nearest Cr-neighbors of the alloying atom and E_{nn} is the nearest neighbor interaction energy from table 3. Using the value of E_{nn} calculated from a magnetic matrix results in numbers that differ strongly for the three non-nn-cells.

However, because the $Ni_{25}Cr_6X$ cells have rather low magnetic moments and the energy difference between non-nn-cell 1 and 2 is close to the nonmagnetic nearest neighbour interaction energy, we can use the nonmagnetic interaction energy instead. Doing this results in more consistent values for the for elements Al, Ti, Nb, and Ta. All values are negative, showing that the energy of the $Ni_{25}Cr_6X$ cell is lower than expected from a purely nonmagnetic nearest-neighbor repulsion.

As mentioned above, the transfer energy of $Ni_{25}Cr_6X$ is consistently lower in SQS 2 than in SQS 1 by about 120 meV–160 meV. (This is also true for the total energy of these

Preprints (www.preprints.org) | NOT PEER-REVIEWED | Posted: 8 July 2022 doi:10.20944/preprints202207.0128.v1

Table 4. Energy $E_{\text{Cr-rich,X}}$ to transfer an element from a pure nickel matrix to a $Ni_{25}Cr_6X$ cell. Also shown are the number of Cr nearest neighbors in each configuration and the energy $E_{\text{Cr-rich,X, nn}}$ that accounts for nearest neighbor effects, using both magnetic and nonmagnetic interaction energies from table 3. All energies are given in meV.

	$E_{\text{Cr-rich,X}}$				
	non-nn-cell-1	non-nn-cell-2	non-nn-cell-3	SQS-1	SQS-2
Al	252	519	744	332	192
Ti	374	715	1243	384	211
Co	210	224	236	164	223
Nb	324	688	1284	297	132
Ta	368	728	1321	337	164
	$E_{\text{Co-rich,X, nn}}$ with magnetic nn interaction				
	non-nn-cell-1	non-nn-cell-2	non-nn-cell-3	SQS-1	SQS-2
number nn	2	3	4	2	2
Al	-29	98	182	52	-89
Ti	64	251	623	74	-98
Co	198	206	213	152	212
Nb	32	250	699	4	-160
Ta	48	247	681	17	-156
	$E_{\text{Co-rich,X, nn}}$ with non-magnetic nn interaction				
	non-nn-cell-1	non-nn-cell-2	non-nn-cell-3	SQS-1	SQS-2
Al	-289	-293	-338	-209	-349
Ti	-369	-399	-243	-359	-531
Co	280	328	376	233	293
Nb	-547	-618	-458	-574	-739
Ta	-524	-612	-464	-555	-729

cells because the energy of $Ni_{26}Cr_6$ SQS 1 and SQS 2 is almost the same.) A closer look at the cells (Figure 3) shows that SQS 2 contains a plane of Ni atoms next to a chain of Cr atoms. This structure can be expected to be under tensile strain. Due to these strains, this plane can accomodate an alloying atom of larger radius more easily than SQS 1. However, since the overall magnetic moment of all SQS 2 cells is larger than that of SQS 1, magnetic effects may also lower the energy of SQS 2 relative to SQS 1. To discern these effects, we performed non-spin-polarized calculations for the two SQS cells. In the non-polarized cells, the total energy of $Ni_{25}Cr_6X$ is lower for SQS 2 than SQS 1 for the elements Ti, Nb, and Ta, but almost identical for Al, and the difference is smaller than before (between 100 meV and 130 meV). Thus, both magnetic and elastic effects are responsible for the lower energy of the SQS 2 $Ni_{25}Cr_6X$ cells. That the $Ni_{26}Cr_6$ SQS 2 is very close in energy to SQS 1 is due to the cancellation of two effects: the large elastic strains in the Ni planes increase the energy, but the stronger magnetic interaction lowers it.

In summary, the results show that the effect of a high Cr content on the solution energy of Al, Ti, Nb, and Ta is complex. The nearest-neighbor repulsion is larger in a situation without spin polarization. Since increasing the Cr content reduces the magnetic effects, it can be expected that the repulsion between Cr and the alloying elements increases as well. Since the repulsion in a non spin-polarized calculation correlates well with the atomic volume, the energy seems to be dominated by elastic effects. The final energy is lower than predicted by the purely non-magnetic interaction.

For Co, the transfer energy $E_{\text{Cr-rich,Co}}$ is about 200 meV for all configurations. Taking the nearest-neighbor interaction energy into account does not change this number significantly since the interaction energy is rather small. As the ionic radius of Co is very close to that of Ni, elastic effects can be expected to be small. To test this, some calculations without relaxation were performed, confirming that ionic relaxation due to Co is small.

On the other hand, Co has a large magnetic moment when placed in a Ni matrix, whereas the Cr-rich cells have low magnetic moments. This suggests that the effect of a

Preprints (www.preprints.org) | NOT PEER-REVIEWED | Posted: 8 July 2022 doi:10.20944/preprints202207.0128.v1

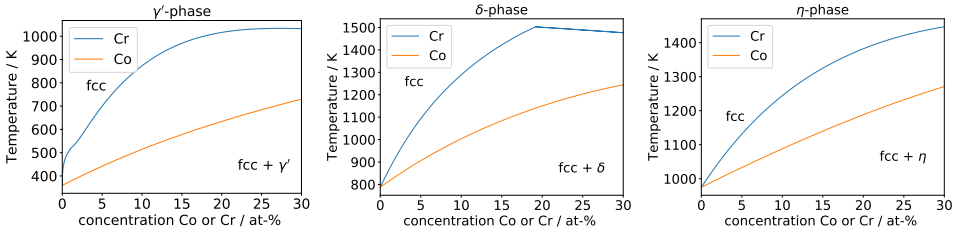

Figure 5. Pseudobinary phase diagrams showing the solvus lines of the phases γ', δ, η as a function of the Cr or Co content. The alloy composition at 0% is Ni 5 at-% Al for γ', Ni 8 at-% Nb for δ and Ni 8 at-% Ti for η. The kink in the line for the δ-phase is due to the solvus line meeting the solidus line.

Cr-rich matrix is due to magnetic interactions. To check this, we calculated the energy difference between a Co atom in a magnetic Ni matrix to that in a non-magnetic Ni matrix. This difference is 310 meV, about 100 meV larger than $E_{\text{Cr-rich,Co}}$ and close to the values of $E_{\text{Cr-rich,Co,nn}}$ when using the nonmagnetic interaction energy. Some deviations are to be expected because Co does retain some magnetic moment in the $Ni_{25}Cr_6Co$ cell.

To further confirm this picture, we simulated the two SQS structures without spin polarization. In this case, $E_{\text{Cr-rich,Co}}$ is rather small with values of 72 meV and 59 meV. Taking the nonmagnetic nearest-neighbor interaction into account to calculate $E_{\text{Cr-rich,Co,nn}}$ for the nonmagnetic case results in very small values of 2 meV and 10 meV. Thus, in the non-magnetic case, the energy is predicted very well.

In conclusion, Co has a higher energy in a Cr-rich matrix because the magnetic interactions, which lower the energy of Co in pure Ni, are disturbed, whereas elastic effects do not play a significant role.

4. Discussion

It was shown in the previous section that both Co and Cr increase the energy of the phase-forming elements (Al, Ti, Nb, Ta) in the nickel matrix and thus may stabilize the respective phases. The effect of Co is mainly due to the direct interaction energy between Co and an alloying element in the nearest-neighbor position. For Cr, interaction energies are generally higher, especially if nonmagnetic nearest-neighbor interactions are considered as is appropriate for high Cr content. In cells where the Cr content is large, the energy is not as large as expected by the direct nearest-neighbor interaction.

From this it can be concluded that the solvus temperature of the phases considered should increase with the Co and Cr content. Since the effect is simply cumulative for Co (the number of nearest-neighbor bonds of an alloying atom directly determine the energy increase), it can be expected that this increase should be almost linear.

For Cr, on the other hand, interaction energies are larger so it should be expected that the slope of the solvus line is larger than for Co. Furthermore, since the increase in energy is not directly proportional to the number of bonds and is lower than expected at high concentrations (if nonmagnetic interaction energies are considered), the slope of the line should decrease with increasing concentration.

To confirm this, simple thermodynamical calculations with the software Thermocalc [19] using the TTNI8 database were performed. We calculated pseudobinary phase diagrams, excluding all phases except for fcc, liquid, and the phase under consideration. The basic alloy composition at 0% was chosen as Ni 5 at-% Al for γ', Ni 8 at-% Nb for δ and Ni 8 at-% Ti for η. Phase boundaries were calculated for a Co or Cr content up to 30 at-%.

The results of the calculation are shown in Figure 5. The solvus lines behave as expected, with a lower slope and a more linear shape for Co and an initially higher slope and a more curved shape for Cr. For the γ'-phase, it should be noted that Thermocalc predicts that Cr preferentially dissolves in γ', so this solvus line does not capture a displacing effect, but rather a direct stabilization of the phase. For Co in γ' and both for Co and Cr in δ and η, Thermocalc predicts low solubility so the solvus line should mainly represent the energy increase of the element in a matrix rich in Co or Cr.

The conclusions drawn here from our simulations are also supported by experimental findings. Heslop [20] determined the γ'-solvus temperatures in the two model alloys Ni-20Cr-xTi-(x/2)Al and Ni-20Cr-20Co-xTi-(x/2)l. At 2%Ti (i. e. 1%Al) he found solvus temperatures of about 820 °C and 910 °C for the former and latter alloy, respectively. However, it should be noted that the difference diminished with increasing Ti-content and eventually turned around at about 5% Ti. This illustrates again that concentration-dependent effects may occur. Also, further interactions may take place in multi-component alloys not considered here. In [8,21,22], a new Nb-containing wrought superalloy was developed. In this context, it was found that Co-addition increases the solvus temperature of the Nb-rich high temperature precipitates that were identified to consist of η- and δ-phase [23].

The results of the DFT calculations also show that a high Cr content increases the energy of Co by about 200 meV. According to [5,6], the energy needed to transfer Co from a pure nickel matrix to the γ''- or δ-phase is approximately 300 meV. This energy is thus significantly reduced when Cr is present in the Ni matrix, so it can be expected that at least some Co will be found in the γ''- or δ-phase.

To summarize, we have studied the effect of high Co or Cr content on the solution energy of important alloying elements in a nickel matrix. Both Co and Cr increase the solution energy and can thus be expected to increase the solvus temperature of the phases. For Co, this is explained by the nearest-neighbor interaction. For Cr, there is a more complex interplay between the direct interaction between the atoms and a change in the overall magnetic state of the alloy.

Author Contributions: Conceptualization, M.B. and J.R.; methodology, M.B.; validation, M.B.; writing—original draft preparation, M.B.; writing—review and editing, M.B. and J.R.; supervision, J.R.; project administration, M.B.; funding acquisition, M.B. and J.R. . All authors have read and agreed to the published version of the manuscript.

Funding: This research was partially funded by the Deutsche Forschungsgemeinschaft grant DFG BA 1795/13-1. Computations were performed at the Hochleistungsrechenzentrum Norddeutschland under grant nic00029. We acknowledge support by the Open Access Publication Funds of Technische Universität Braunschweig.

Data Availability Statement: Data available on request

Acknowledgments: Thanks to Martin Bergner for help in setting up the Thermocalc calculations.

Conflicts of Interest: The authors declare no conflict of interest.

1. Schilke, P.W.; Pepe, J.; Schwant, R.C. Alloy 706 metallurgy and turbine wheel application. *Superalloys* **1994**, *718*, 1.
2. Woodward, C.; Van De Walle, A.; Asta, M.; Trinkle, D. First-principles study of interfacial boundaries in Ni–Ni3Al. *Acta materialia* **2014**, *75*, 60–70.
3. Wu, X.; Wang, C. Density functional theory study of the thermodynamic and elastic properties of Ni-based superalloys. *Journal of Physics: Condensed Matter* **2015**, *27*, 295401.
4. Eriş, R.; Akdeniz, M.V.; Mekhrabov, A.O. The site preferences of transition elements and their synergistic effects on the bonding strengthening and structural stability of γ'-Ni3Al precipitates in Ni-based superalloys: a first-principles investigation. *Metallurgical and Materials Transactions A* **2021**, *52*, 2298–2313.
5. Bäker, M.; Rösler, J.; Hentrich, T.; Ackland, G. Influence of transition group elements on the stability of the δ-and η-phase in nickelbase alloys. *Modelling and Simulation in Materials Science and Engineering* **2017**, *26*, 015005.
6. Bäker, M.; Rösler, J. Influence of transition group elements on the stability of the γ''-phase in nickelbase alloys. *Modelling and Simulation in Materials Science and Engineering* **2021**, *29*, 055006.
7. Hammerschmidt, T.; Rogal, J.; Bitzek, E.; Drautz, R. Atomic-scale modeling of superalloys. In *Nickel Base Single Crystals Across Length Scales*; Elsevier, 2022; pp. 341–360.
8. Rösler, J.; Hentrich, T.; Gehrmann, B. On the Development Concept for a New 718-Type Superalloy with Improved Temperature Capability. *Metals* **2019**, *9*, 1130.

 doi:10.20944/preprints202207.0128.v1

9. Kresse, G.; Hafner, J. Ab initio molecular-dynamics simulation of the liquid-metal–amorphous-semiconductor transition in germanium. *Physical Review B* **1994**, *49*, 14251.
10. Kresse, G.; Furthmüller, J. Efficient iterative schemes for ab initio total-energy calculations using a plane-wave basis set. *Physical Review B* **1996**, *54*, 11169.
11. Kresse, G.; Furthmüller, J. Efficiency of ab-initio total energy calculations for metals and semiconductors using a plane-wave basis set. *Computational Materials Science* **1996**, *6*, 15–50.
12. Blöchl, P.E. Projector augmented-wave method. *Physical Review B* **1994**, *50*, 17953.
13. Kresse, G.; Joubert, D. From ultrasoft pseudopotentials to the projector augmented-wave method. *Physical Review B* **1999**, *59*, 1758.
14. Birch, F. Finite elastic strain of cubic crystals. *Physical Review* **1947**, *71*, 809.
15. Van De Walle, A. Multicomponent multisublattice alloys, nonconfigurational entropy and other additions to the Alloy Theoretic Automated Toolkit. *Calphad* **2009**, *33*, 266–278.
16. Grau-Crespo, R.; Hamad, S.; Catlow, C.R.A.; De Leeuw, N. Symmetry-adapted configurational modelling of fractional site occupancy in solids. *Journal of Physics: Condensed Matter* **2007**, *19*, 256201.
17. Ding, J.; Yu, Q.; Asta, M.; Ritchie, R.O. Tunable stacking fault energies by tailoring local chemical order in CrCoNi medium-entropy alloys. *Proceedings of the National Academy of Sciences* **2018**, *115*, 8919–8924.
18. Lu, Y.; Jia, D.; Hu, T.; Chen, Z.; Zhang, L. Phase-field study the effects of elastic strain energy on the occupation probability of Cr atom in Ni–Al–Cr alloy. *Superlattices and Microstructures* **2014**, *66*, 105–111.
19. Andersson, J.O.; Helander, T.; Höglund, L.; Shi, P.; Sundman, B. Thermo-Calc & DICTRA, computational tools for materials science. *Calphad* **2002**, *26*, 273–312.
20. Heslop, J. Wrought nickel–chromium heat-resisting alloys containing cobalt. *Cobalt* **1964**, *24*, 128.
21. Fedorova, T.; Rösler, J.; Klöwer, J.; Gehrmann, B. Development of a new 718-type Ni-Co superalloy family for high temperature applications at 750 C. In Proceedings of the MATEC web of conferences. EDP Sciences, 2014, Vol. 14, p. 01003.
22. Fedorova, T.; Rösler, J.; Gehrmann, B.; Klöwer, J. Invention of a New 718-Type Ni-Co Superalloy Family for High Temperature Applications at 750 C. In Proceedings of the 8th International Symposium on Superalloy 718 and Derivatives. Wiley Online Library, 2014, pp. 587–599.
23. Ghica, C.; Solís, C.; Munke, J.; Stark, A.; Gehrmann, B.; Bergner, M.; Rösler, J.; Gilles, R. HRTEM analysis of the high-temperature phases of the newly developed high-temperature Ni-base superalloy VDM 780 Premium. *Journal of alloys and compounds* **2020**, *814*, 152157.